CLEO CONF 96-10
ICHEP96 PA05-072

Search for the Decays $B^0 \to D^{(*)+} D^{(*)-}$

CLEO Collaboration

(July 12, 1996)

Abstract

Using the CLEO II data set we have carried out a search for the Cabbibo-suppressed decays $B^0 \to D^{(*)+} D^{(*)-}$. For the decay $B^0 \to D^{*+} D^{*-}$ we observe one candidate signal event where the expected background is 0.022 ± 0.011 events. Converting this to an upper limit on the branching fraction, one gets $\mathcal{B}(B^0 \to D^{*+} D^{*-}) < 2.5 \times 10^{-3}$ at the 90% CL. For $B^0 \to (D^{*+} D^- + D^+ D^{*-})$ and $B^0 \to D^+ D^-$, no significant excess of signal above the expected background level is seen, and we calculate the upper limits at 90% CL on the branching fractions to be $\mathcal{B}(B^0 \to (D^{*+} D^- + D^+ D^{*-})) < 2.0 \times 10^{-3}$ and $\mathcal{B}(B^0 \to D^+ D^-) < 1.3 \times 10^{-3}$.

M. Bishai,[1] J. Fast,[1] E. Gerndt,[1] J. W. Hinson,[1] D. H. Miller,[1] E. I. Shibata,[1]
I. P. J. Shipsey,[1] M. Yurko,[1] L. Gibbons,[2] S. D. Johnson,[2] Y. Kwon,[2] S. Roberts,[2]
E. H. Thorndike,[2] C. P. Jessop,[3] K. Lingel,[3] H. Marsiske,[3] M. L. Perl,[3] S. F. Schaffner,[3]
D. Ugolini,[3] R. Wang,[3] X. Zhou,[3] T. E. Coan,[4] V. Fadeyev,[4] I. Korolkov,[4] Y. Maravin,[4]
I. Narsky,[4] V. Shelkov,[4] R. Stroynowski,[4] J. Staeck,[4] I. Volobouev,[4] J. Ye,[4] M. Artuso,[5]
A. Efimov,[5] M. Gao,[5] M. Goldberg,[5] R. Greene,[5] F. Frasconi,[5] D. He,[5] S. Kopp,[5]
G. C. Moneti,[5] R. Mountain,[5] Y. Mukhin,[5] S. Schuh,[5] T. Skwarnicki,[5] S. Stone,[5] X. Xing,[5]
J. Bartelt,[6] S. E. Csorna,[6] V. Jain,[6] S. Marka,[6] A. Freyberger,[7] R. Godang,[7] D. Gibaut,[7]
K. Kinoshita,[7] I. C. Lai,[7] P. Pomianowski,[7] S. Schrenk,[7] G. Bonvicini,[8] D. Cinabro,[8]
L. Perera,[8] B. Barish,[9] M. Chadha,[9] S. Chan,[9] G. Eigen,[9] J. S. Miller,[9] C. O'Grady,[9]
M. Schmidtler,[9] J. Urheim,[9] A. J. Weinstein,[9] F. Würthwein,[9] D. M. Asner,[10]
D. W. Bliss,[10] W. S. Brower,[10] G. Masek,[10] H. P. Paar,[10] J. Gronberg,[11] C. M. Korte,[11]
D. J. Lange,[11] R. Kutschke,[11] S. Menary,[11] R. J. Morrison,[11] S. Nakanishi,[11]
H. N. Nelson,[11] T. K. Nelson,[11] C. Qiao,[11] J. D. Richman,[11] D. Roberts,[11] A. Ryd,[11]
H. Tajima,[11] M. S. Witherell,[11] R. Balest,[12] B. H. Behrens,[12] K. Cho,[12] W. T. Ford,[12]
H. Park,[12] P. Rankin,[12] J. Roy,[12] J. G. Smith,[12] J. P. Alexander,[13] C. Bebek,[13]
B. E. Berger,[13] K. Berkelman,[13] K. Bloom,[13] D. G. Cassel,[13] H. A. Cho,[13]
D. M. Coffman,[13] D. S. Crowcroft,[13] M. Dickson,[13] P. S. Drell,[13] R. Ehrlich,[13] R. Elia,[13]
A. D. Foland,[13] P. Gaidarev,[13] B. Gittelman,[13] S. W. Gray,[13] D. L. Hartill,[13]
B. K. Heltsley,[13] P. I. Hopman,[13] S. L. Jones,[13] J. Kandaswamy,[13] N. Katayama,[13]
P. C. Kim,[13] D. L. Kreinick,[13] T. Lee,[13] Y. Liu,[13] G. S. Ludwig,[13] J. Masui,[13]
J. Mevissen,[13] N. B. Mistry,[13] C. R. Ng,[13] E. Nordberg,[13] M. Ogg,[13,*] J. R. Patterson,[13]
D. Peterson,[13] D. Riley,[13] A. Soffer,[13] C. Ward,[13] P. Avery,[14] M. Athanas,[14] C. D. Jones,[14]
M. Lohner,[14] C. Prescott,[14] S. Yang,[14] J. Yelton,[14] J. Zheng,[14] G. Brandenburg,[15]
R. A. Briere,[15] D. Y.-J. Kim,[15] T. Liu,[15] M. Saulnier,[15] R. Wilson,[15] H. Yamamoto,[15]
T. E. Browder,[16] F. Li,[16] Y. Li,[16] J. L. Rodriguez,[16] T. Bergfeld,[17] B. I. Eisenstein,[17]
J. Ernst,[17] G. E. Gladding,[17] G. D. Gollin,[17] E. Johnson,[17] I. Karliner,[17] M. Palmer,[17]
M. Selen,[17] J. J. Thaler,[17] K. W. Edwards,[18] A. Bellerive,[19] D. I. Britton,[19] R. Janicek,[19]
D. B. MacFarlane,[19] K. W. McLean,[19] P. M. Patel,[19] A. J. Sadoff,[20] R. Ammar,[21]
P. Baringer,[21] A. Bean,[21] D. Besson,[21] D. Coppage,[21] C. Darling,[21] R. Davis,[21]
N. Hancock,[21] S. Kotov,[21] I. Kravchenko,[21] N. Kwak,[21] S. Anderson,[22] Y. Kubota,[22]
M. Lattery,[22] J. J. O'Neill,[22] S. Patton,[22] R. Poling,[22] T. Riehle,[22] A. Smith,[22]
V. Savinov,[22] M. S. Alam,[23] S. B. Athar,[23] Z. Ling,[23] A. H. Mahmood,[23] H. Severini,[23]
S. Timm,[23] F. Wappler,[23] A. Anastassov,[24] S. Blinov,[24,†] J. E. Duboscq,[24] R. Fulton,[24]
D. Fujino,[24] K. K. Gan,[24] T. Hart,[24] K. Honscheid,[24] H. Kagan,[24] R. Kass,[24] J. Lee,[24]
M. Sung,[24] A. Undrus,[24,†] R. Wanke,[24] A. Wolf,[24] M. M. Zoeller,[24] B. Nemati,[25]
S. J. Richichi,[25] W. R. Ross,[25] P. Skubic,[25] and M. Wood[25]

[1]Purdue University, West Lafayette, Indiana 47907
[2]University of Rochester, Rochester, New York 14627

---

[*]Permanent address: University of Texas at Austin.

[†]Permanent address: BINP, RU-630090 Novosibirsk, Russia.

[3]Stanford Linear Accelerator Center, Stanford University, Stanford, California 94309
[4]Southern Methodist University, Dallas, Texas 75275
[5]Syracuse University, Syracuse, New York 13244
[6]Vanderbilt University, Nashville, Tennessee 37235
[7]Virginia Polytechnic Institute and State University, Blacksburg, Virginia 24061
[8]Wayne State University, Detroit, Michigan 48202
[9]California Institute of Technology, Pasadena, California 91125
[10]University of California, San Diego, La Jolla, California 92093
[11]University of California, Santa Barbara, California 93106
[12]University of Colorado, Boulder, Colorado 80309-0390
[13]Cornell University, Ithaca, New York 14853
[14]University of Florida, Gainesville, Florida 32611
[15]Harvard University, Cambridge, Massachusetts 02138
[16]University of Hawaii at Manoa, Honolulu, Hawaii 96822
[17]University of Illinois, Champaign-Urbana, Illinois 61801
[18]Carleton University, Ottawa, Ontario, Canada K1S 5B6
and the Institute of Particle Physics, Canada
[19]McGill University, Montréal, Québec, Canada H3A 2T8
and the Institute of Particle Physics, Canada
[20]Ithaca College, Ithaca, New York 14850
[21]University of Kansas, Lawrence, Kansas 66045
[22]University of Minnesota, Minneapolis, Minnesota 55455
[23]State University of New York at Albany, Albany, New York 12222
[24]Ohio State University, Columbus, Ohio 43210
[25]University of Oklahoma, Norman, Oklahoma 73019

I. INTRODUCTION

The primary physics motivation for studying the decays $B^0 \to D^{(*)+} D^{(*)-}$ is that they are favorable modes for testing CP violation in B decays. Time-dependent asymmetries in the decays can be related to the angle β of the unitarity triangle [1]. Although $B^0 \to D^{*+} D^{*-}$ and $B^0 \to (D^{*+} D^- + D^+ D^{*-})$ are not pure CP eigenstates, estimates indicate that a dilution of the CP asymmetry of only a few percent would be incurred by treating these modes as pure CP eigenstates [1]. The sensitivity for measuring $\sin 2\beta$ in $B^0 \to D^{(*)+} D^{(*)-}$ could be comparable to that obtained by using $B^0 \to J/\psi K^0_S$ [2,3].

The modes $B^0 \to D^{(*)+} D^{(*)-}$ have never been observed, and no published limits on their branching fractions exist. The decay amplitude is dominated by a W spectator diagram with $\bar{b} \to \bar{c} W^+$ followed by the Cabbibo-suppressed $W^+ \to c\bar{d}$. One can estimate the branching fractions by relating $B^0 \to D^{(*)+} D^{(*)-}$ to the Cabibbo-favored decays $B^0 \to D_s^{(*)+} D^{(*)-}$:

$$\mathcal{B}(B^0 \to D^{(*)+} D^{(*)-}) \simeq \left(\frac{f_{D^{(*)}}}{f_{D_s^{(*)}}}\right)^2 \cdot \tan^2(\theta_c) \cdot \mathcal{B}(B^0 \to D_s^{(*)+} D^{(*)-}) \tag{1}$$

$$\simeq (0.9)^2 \cdot (1/20) \cdot \mathcal{B}(B^0 \to D_s^{(*)+} D^{(*)-}) \tag{2}$$

Table I shows the expected $B^0 \to D^{(*)+} D^{(*)-}$ branching fractions where the CLEO measurements of $\mathcal{B}(B^0 \to D_s^{(*)+} D^{(*)-})$ have been used [4].

TABLE I. Estimated branching fractions for $B^0 \to D^{(*)+} D^{(*)-}$ based on the measured branching fractions of the Cabibbo favored decays $B^0 \to D_s^{(*)+} D^{(*)-}$.

Mode	$\mathcal{B}$ of related $D_s^{(*)+} D^{(*)-}$ Mode	Estimated $\mathcal{B}$
$B^0 \to D^{*+} D^{*-}$	2.4%	0.097%
$B^0 \to (D^{*+} D^- + D^+ D^{*-})$	2.0%	0.081%
$B^0 \to D^+ D^-$	1.1%	0.045%

II. DATA SAMPLE AND EVENT SELECTION

The data used in this analysis were recorded with the CLEO-II detector [5] located at the Cornell Electron Storage Ring (CESR). An integrated luminosity of 3.09 fb^{-1} was taken at the Υ(4S) resonance, corresponding to approximately $(3.32 \pm 0.06) \times 10^6$ $B\overline{B}$ pairs produced.

At the Υ(4S), the $B\overline{B}$ pairs are produced nearly at rest resulting in a spherical event topology. This is in contrast to the continuum events which have a more jet-like topology. To select spherical events, we require that the ratio R_2 of the second and zeroth Fox-Wolfram moments [6] be less than 0.25.

Charged tracks were required to be of good quality and to be consistent with coming from the interaction region in both the $r - \phi$ and $r - z$ planes. Photon candidates were defined to be isolated clusters in the CsI calorimeter with energies greater than 30 MeV in the central region ($\cos\theta \leq 0.71$, where θ is measured from the beamline) and greater than 50 MeV elsewhere. Pairs of photons with invariant mass within 2.5σ of the nominal π^0 mass were used to form π^0 candidates. Selected π^0 candidates were then kinematically fit to the nominal π^0 mass.

A particle identification system consisting of dE/dx and time-of-flight was used to distinguish charged kaons from charged pions. For charged pion candidates, the likelihood of the pion hypothesis, L_π, is required to be greater than 0.05. Since all signal modes require two charged kaons, the kaon candidates were required to have a joint kaon hypothesis likelihood, $L_{K_1} \cdot L_{K_2}$, greater than 0.10.

All D^{*+}s are reconstructed in the mode $D^{*+} \to \pi^+ D^0$ (charge-conjugate modes are implied). D^0 candidates are reconstructed in the modes $D^0 \to K^+ \pi^-$, $D^0 \to K^+ \pi^- \pi^0$ and $D^0 \to K^+ \pi^- \pi^+ \pi^-$. And D^+ candidates are reconstructed via $D^+ \to K^- \pi^+ \pi^+$. Table II summarizes the branching fractions of the $D^{(*)}$ modes used.

TABLE II. Branching fractions of $D^{(*)}$ modes used in reconstruction.

Particle	Decay Modes	Branching Fraction
D^{*+}	$D^{*+} \to \pi^+ D^0$	$(68.1 \pm 1.6)\%$
D^0	$D^0 \to K^+ \pi^-$	$(3.91 \pm 0.19)\%$
	$D^0 \to K^+ \pi^- \pi^0$	$(12.1 \pm 1.1)\%$
	$D^0 \to K^+ \pi^- \pi^+ \pi^-$	$(8.0 \pm 0.5)\%$
D^+	$D^+ \to K^- \pi^+ \pi^+$	$(9.1 \pm 1.4)\%$

A vertex-constrained fit was performed on all the charged tracks in the B^0 candidate for modes that contained a D^{*+}. The fit provided an improved measurement of the angular track parameters for the slow π^+ from the D^{*+} decay. The resulting r. m. s. resolution on $\Delta m_{D^*-D} \equiv m_{D^{*+}} - m_{D^0}$ is approximately 0.69 MeV. Figure 1 shows Δm_{D^*-D} for inclusive D^*s in the momentum range expected for the $B^0 \to D^{(*)+} D^{(*)-}$ decays. The χ^2 from the vertex fit was required to be less than 100.

The $B^0 \to (D^{*+} D^- + D^+ D^{*-})$ is an example of a $Pseudoscalar \to Vector + Pseudoscalar$ decay. The cosine of the decay angle of the slow π^+ from the D^{*+} has a $\cos^2\theta_{Helicity}$ distribution. Background events have a flat distribution in this variable. $B^0 \to (D^{*+} D^- + D^+ D^{*-})$ candidates were required to have $|\cos\theta_{Helicity}| > 0.5$.

A mass χ^2 (χ^2_M) was constructed that included the various reconstructed $D^{(*)}$ masses for the B^0 candidate. For example, in $B^0 \to D^{*+} D^{*-}$ the χ^2_M included a measured Δm_{D^*-D} and a measured m_{D^0} from each D^* for a total of four terms. The χ^2_M cuts chosen for each mode are summarized in Table III. Backgrounds are flat in χ^2_M.

Since the energy of the B^0 is equal to the beam energy, we use the beam energy instead of the measured energy of the B^0 candidate to calculate the beam-constrained mass: $m_B = \sqrt{E^2_{beam} - \mathbf{p}^2_B}$, where $\mathbf{p}^2_B$ is the measured momentum of the B^0 candidate. The r. m. s. resolution in m_B for signal events, as determined from Monte Carlo, is 2.8 MeV. In addition, the energy difference, $\Delta E \equiv E_B - E_{beam}$, where E_B is the measured B^0 energy, was used to distinguish signal from background. The resolution in ΔE is about 12 MeV after performing a mass-constrained fit that

TABLE III. χ^2_M cuts chosen for each mode. The number in parenthesis in the subscript indicates the number of mass terms included in the χ^2_M.

Mode	χ^2_M Cut
$B^0 \to D^{*+} D^{*-}$	$\chi^2_{M(4)} < 8.0$
$B^0 \to (D^{*+} D^- + D^+ D^{*-})$	$\chi^2_{M(3)} < 4.0$
$B^0 \to D^+ D^-$	$\chi^2_{M(2)} < 2.0$

included the masses of all secondary particles ($D^{(*)}$s and π^0s). The signal region in all modes was defined as $|\Delta E| < 2\sigma_{\Delta E}$ and $|m_B - \overline{m_{B^0}}| < 2\sigma_{m_B}$.

All cuts were tuned exclusively on Monte Carlo events. Since the number of observed signal events was expected to be small, all cuts were optimized to minimize the probability that the expected background level would fluctuate up to or beyond the expected signal level. For the purposes of cut tuning, when calculating the expected number of signal events a branching fraction of 0.1% was assumed for all $B^0 \to D^{(*)+} D^{(*)-}$ modes.

III. SIGNAL EFFICIENCY AND SINGLE EVENT SENSITIVITY

Using the cuts defined above, the signal efficiency was determined using Monte Carlo. The efficiency and single event sensitivity ($SES \equiv (\epsilon \cdot \mathcal{B} \cdot N_{B\overline{B}})^{-1}$) for each mode are summarized in Table IV. The systematic uncertainty on the SES is dominated largely by uncertainties in the D and D^* branching fractions, and, due to the large mean multiplicity of the final states, the uncertainty in the tracking efficiency.

TABLE IV. Summary of Monte Carlo determined efficiencies for the three $B^0 \to D^{(*)+} D^{(*)-}$ modes. Also quoted is the single event sensitivity, and, using the predicted branching fractions in Table I, the expected number of observed signal events.

Mode	Efficiency	SES	Predicted Number of Signal Events
$B^0 \to D^{*+} D^{*-}$	1.86%	$(6.07 \pm 1.12) \times 10^{-4}$	1.7
$B^0 \to (D^{*+} D^- + D^+ D^{*-})$	5.07%	$(4.00 \pm 0.78) \times 10^{-4}$	1.8
$B^0 \to D^+ D^-$	14.41%	$(2.53 \pm 0.79) \times 10^{-4}$	2.0

IV. BACKGROUND ESTIMATION

The dominant background is combinatoric background from generic $B\overline{B}$ and continuum events. The Monte Carlo shows that this background varies smoothly in ΔE and m_B . The m_B background distribution for data in ΔE sidebands (50 MeV $\leq |\Delta E| \leq$ 400 MeV) also varies smoothly. The same is true for the ΔE backround distribution for data with $m_B < 5.27$ GeV. To estimate the background in the signal region, we count the events in a sideband in the ΔE-m_B plane (50 MeV $\leq |\Delta E| \leq$ 400 MeV; 5.2 GeV $\leq m_B \leq E_{beam}$) and multiply by the relative efficiencies of the signal and sideband regions determined from background Monte Carlo.

V. DATA AND RESULTS

The above analysis is applied to the data, and the results are shown in Figures 2, 3 and 4, which show plots of ΔE vs. m_B with all other cuts applied. The signal region is indicated with a solid line, and the sideband region is indicated with a dotted line.

Table V gives a summary of the event yields in the sideband and signal regions. The expected number of background events in the signal region is also shown. The uncertainty on the expected number of background events is a combination of statistical error on the number of events in the ΔE sideband regions and the uncertainty in the background shape through the signal region. For $B^0 \to D^{*+} D^{*-}$, this error is dominated by the statistical error in the number of events in the sidebands, but for $B^0 \to (D^{*+} D^- + D^+ D^{*-})$ and $B^0 \to D^+ D^-$ both contributions are roughly equal.

TABLE V. Summary of events found in the data, both in the ΔE sidebands and in the signal region, for each of the three modes.

Mode	Events in ΔE Sidebands	Predicted Background in the Signal Region	Events found in Signal Region
$B^0 \to D^{*+} D^{*-}$	4	0.022 ± 0.011	1
$B^0 \to (D^{*+} D^- + D^+ D^{*-})$	117	0.64 ± 0.10	2
$B^0 \to D^+ D^-$	539	2.64 ± 0.34	3

The probability that the expected background of 0.022 ± 0.011 events in $B^0 \to D^{*+} D^{*-}$ fluctuates up to or exceeds the observed one event is approximately 2.2%. If we interpret this event as evidence for a signal, the resulting branching fraction would be

$$\mathcal{B}(B^0 \to D^{*+} D^{*-}) = [(6.0^{+8.1}_{-4.2}(stat)) \times 10^{-4}] \times [1 \pm 0.18(syst)], \tag{3}$$

where the systematic uncertainty comes from the uncertainty on the SES.

No significant excess of events is seen in the other two modes. We calculate upper limits on the branching fractions for all three modes, and these results are summarized in Table VI. The systematic uncertainty in the SES and the uncertainty in the background level have been incorporated into the upper limits [7].

VI. CONCLUSIONS

We have performed a search for the decays $B^0 \to D^{(*)+} D^{(*)-}$. In the mode $B^0 \to D^{*+} D^{*-}$, one event is seen in the signal region where the expected background is 0.022 ± 0.011. The one event

TABLE VI. Summary of upper limits on the $B^0 \to D^{(*)+} D^{(*)-}$ branching fractions. All upper limits are quoted at the 90% confidence level.

Mode	Upper Limit (90% C. L.)
$B^0 \to D^{*+} D^{*-}$	2.5×10^{-3}
$B^0 \to (D^{*+} D^- + D^+ D^{*-})$	2.0×10^{-3}
$B^0 \to D^+ D^-$	1.3×10^{-3}

in $B^0 \to D^{*+} D^{*-}$ is seen at a rate which is consistent with predictions, and in all three modes the upper limits are within about a factor of two from the predicted branching fractions.

ACKNOWLEDGMENTS

We gratefully acknowledge the effort of the CESR staff in providing us with excellent luminosity and running conditions. J.P.A., J.R.P., and I.P.J.S. thank the NYI program of the NSF, M.S thanks the PFF program of the NSF, G.E. thanks the Heisenberg Foundation, K.K.G., M.S., H.N.N., T.S., and H.Y. thank the OJI program of DOE, J.R.P, K.H., and M.S. thank the A.P. Sloan Foundation, and A.W., and R.W. thank the Alexander von Humboldt Stiftung for support. This work was supported by the National Science Foundation, the U.S. Department of Energy, and the Natural Sciences and Engineering Research Council of Canada.

REFERENCES

[1] R. Aleksan *et al.*, Phys. Lett. **B317**, 173 (1993).
[2] The *BaBar* Collaboration, Technical Design Report, SLAC-R-95-457 (1995).
[3] K. Lingel *et al.*, "Physics Rationale for a B Factory", CLNS 91-1043 (1991).
[4] CLEO Collaboration, D. Gibaut *et al.*, Phys. Rev. D **53**, 4734 (1996).
[5] CLEO Collaboration, Y. Kubota *et al.*, Nucl. Instrum. Methods A **320**, 66 (1992).
[6] G. Fox and S. Wolfram, Phys. Rev. Lett. **41**, 1581 (1978).
[7] R. D. Cousins and V. Highland, Nucl. Instrum. Methods A **320**, 331 (1992).

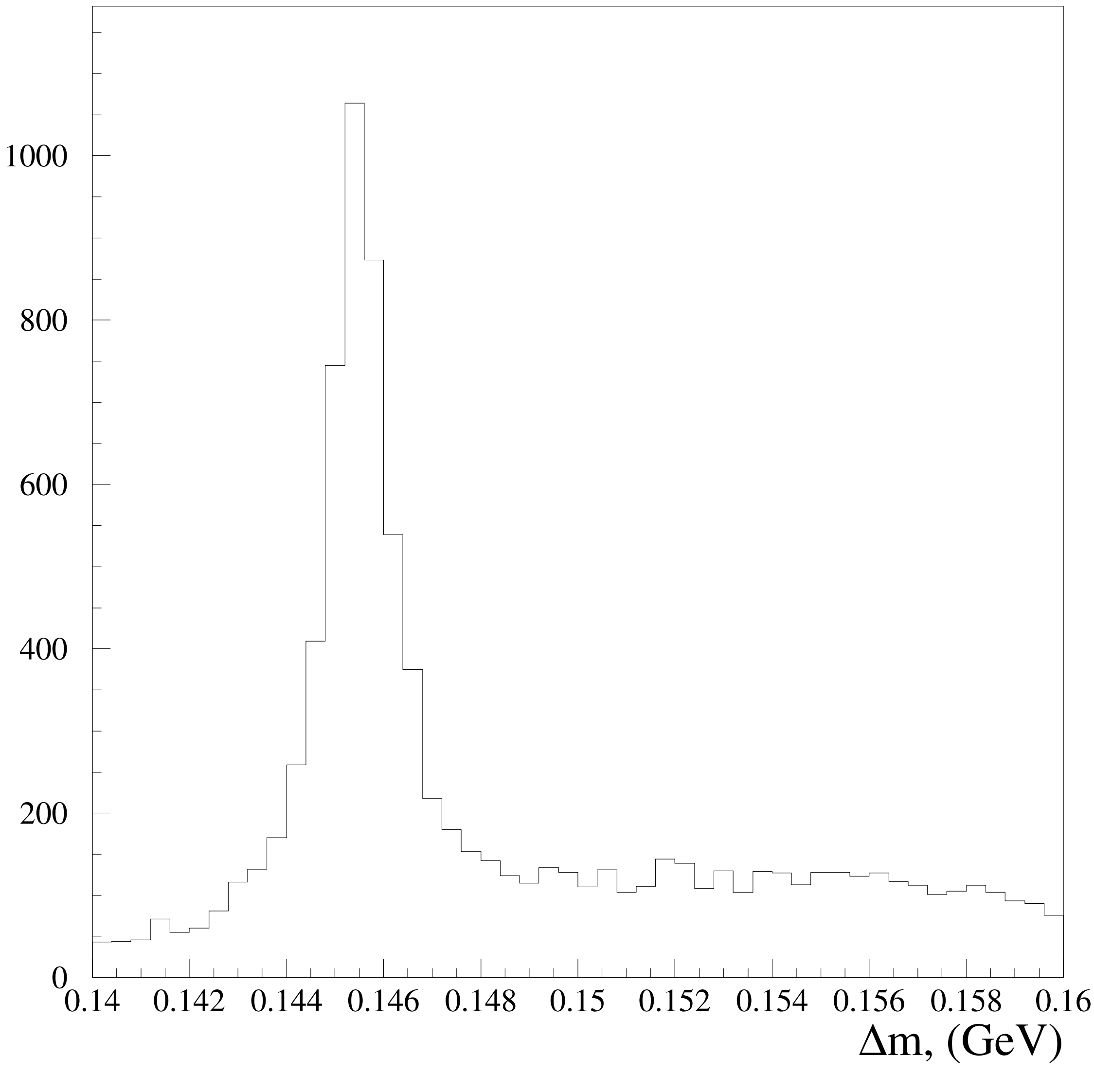

FIG. 1. $\Delta m_{D^{*}-D}$ from data for inclusive D^{*+}s in the momentum range expected from $B^0 \to D^{(*)+} D^{(*)-}$ decays.

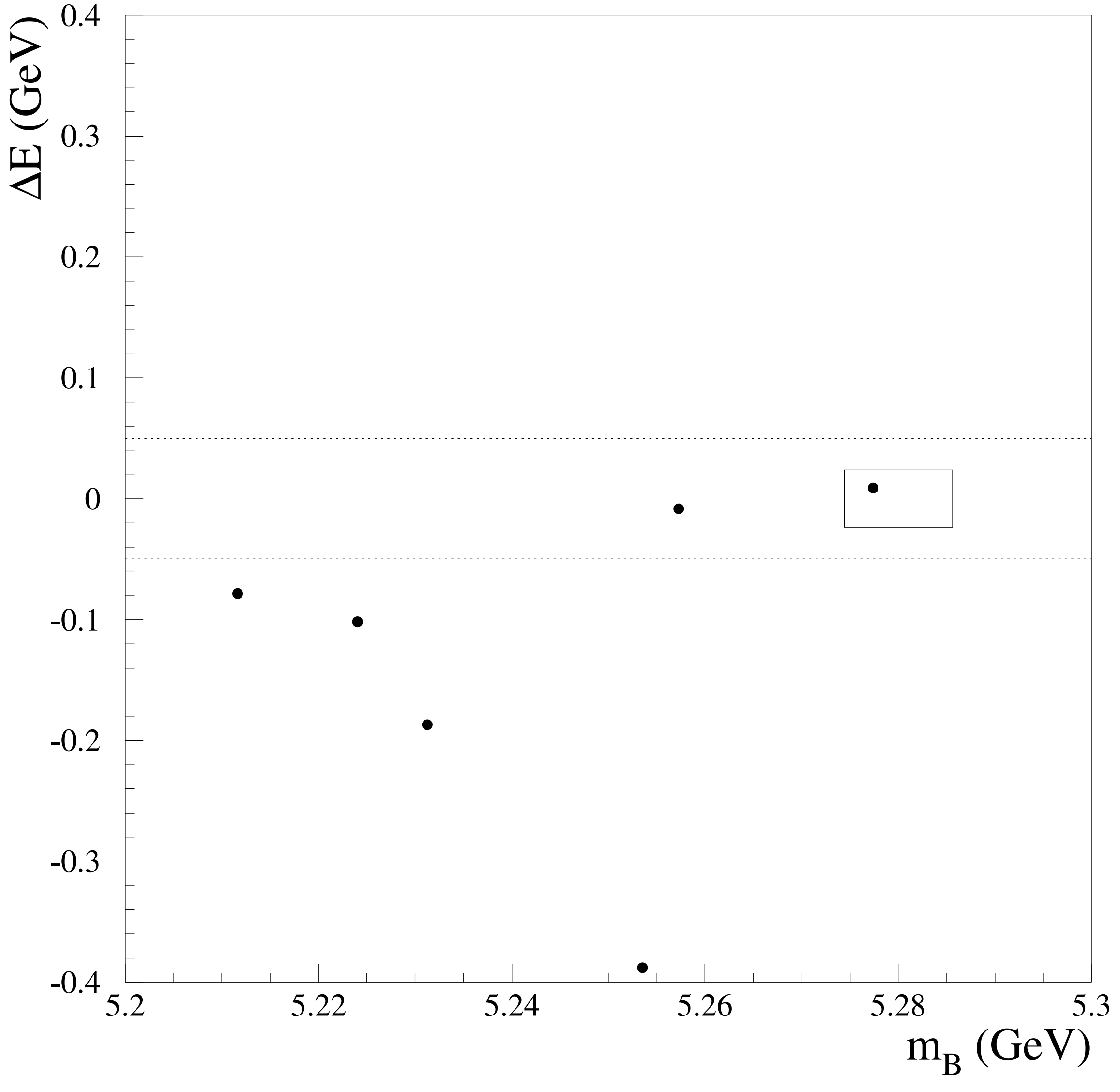

FIG. 2. ΔE vs. m_B for data in the $B^0 \to D^{*+}\, D^{*-}$ analysis. The signal region is indicated by a solid box. The sideband region lies above the top and below the bottom dotted lines.

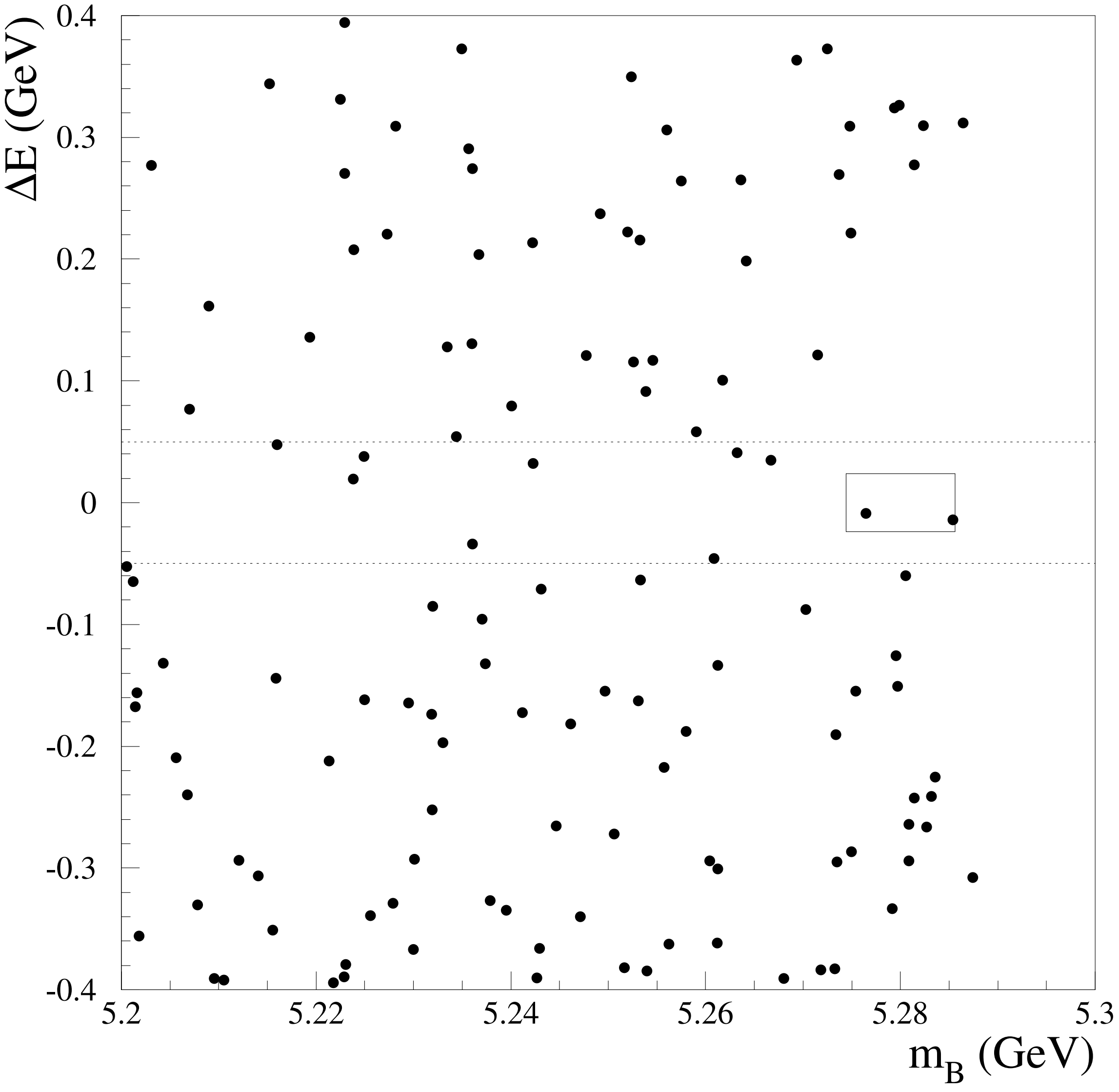

FIG. 3. ΔE vs. m_B for data in the $B^0 \to (D^{*+}\,D^- + D^+\,D^{*-})$analysis. The signal region is indicated by a solid box. The sideband region lies above the top and below the bottom dotted lines.

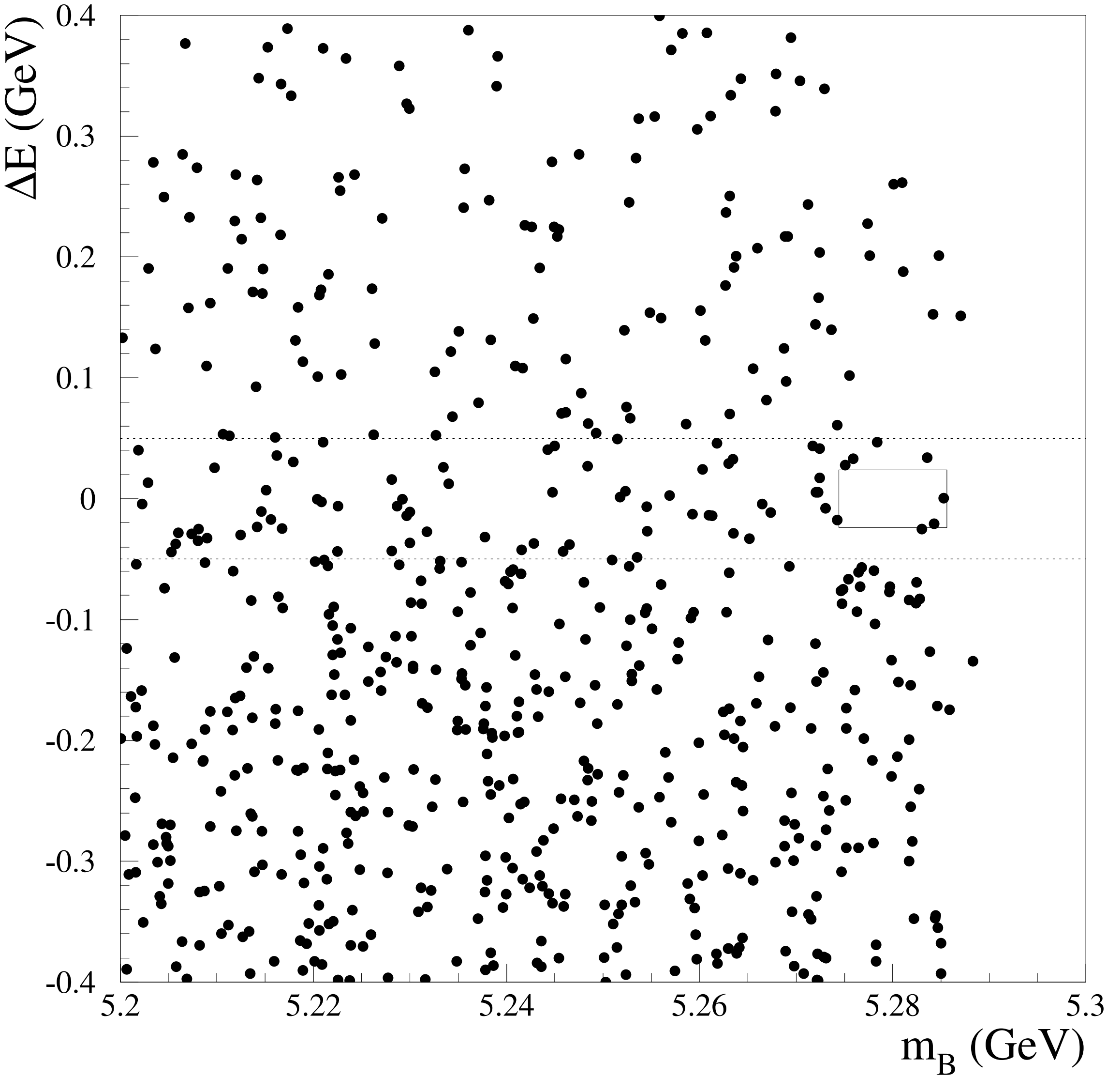

FIG. 4. ΔE vs. m_B for data in the $B^0 \to D^+ D^-$ analysis. The signal region is indicated by a solid box. The sideband region lies above the top and below the bottom dotted lines.